# Glacier melt runoff controls bedload transport in Alpine catchments

**F. Comiti[1], L. Mao[2,3], D. Penna[4], A. Dell'Agnese[1], M. Engel[1], S. Rathburn[5], M. Cavalli [6]**

[1] Faculty of Science and Technology, Free University of Bozen-Bolzano, Piazza Università 5, 39100 Bolzano (Italy).

[2] School of Geography, University of Lincoln, Brayford Pool, Lincoln, LN6 7TS (UK).

[3] Instituto de Geografía, Pontificia Universidad Católica de Chile.

[4] Department of Agriculture, Food, Environment and Forestry, Via S. Bonaventura, 13, University of Florence, 50145 Firenze (Italy).

[5] Department of Geosciences, Colorado State University, 80523 Fort Collins, Colorado (USA).

[6] Research Institute for Geo-Hydrological Protection (IRPI), National Research Council (CNR), Corso Stati Uniti 4, 35127 Padova (Italy).

Corresponding author: Francesco Comiti (francesco.comiti@unibz.it)



## Abstract

Research on factors affecting sediment regime in glacierized catchments under warming climates is still scarce despite its societal relevance. In particular, coarse bedload transport has never been quantitatively related to water runoff origin (snowmelt vs glacier melt), which provides important information on the role of different sediment sources (glaciers vs hillslopes and channel bed). Drawing on data from multiple spatial and temporal scales in a paradigmatic Alpine glacierized catchment, we show that glacier melt flows play a key role in coarse sediment transport dynamics. Bedload concentration measured during glacier melt flows is up to 6 orders of magnitude larger than during snowmelt. At the catchment scale and within the channel, however, minimal aggradation and degradation was detected over almost a decade. In addition, sedimentation rates at a hydropower weir, inferred from flushing frequency during the last four decades, are tightly associated to summer air temperature and not to precipitation trends, and most of sediment export occurred in July-August. However, sediment flushing frequency has been decreasing since the late 1990s despite very warm summers in the following decades. Collectively, these findings indicate that sediment is dominantly sourced from within glacier-covered areas and that transport rates are thus dictated by seasonal and multi-annual glacial dynamics. As glacier melt flows decrease due to ice mass loss, our results suggest that, for similar basins, a progressive shift from supply-limited (driven by glacier activity) to transport-limited (during rainfall-induced events) sediment transport will occur, disrupting the current near-equilibrium channel conditions.

*Keywords: sediment transport, stable water isotopes, glacier retreat, global warming*



## 1 Introduction

The ongoing changes in the cryosphere due to global warming are markedly affecting hydrological regimes in high-elevation mountain catchments (e.g. Beniston et al., 2017; Milner et al. 2017). Over the last decades, snow accumulation at lower elevations has decreased due to higher winter temperatures. Also, snowmelt flows start earlier with peak discharges attenuated in late spring/early summer, whereas glacier melt flows have increased in mid- to late summer (Weber and Prasch, 2016). Abundant research has focused on predicting the future hydrological regimes in different glacierized river basins around the world based on climatic projections. .

Despite the considerable natural variability between years (Kobierska et al., 2013), maximum annual glacier melt runoff is expected to be approaching its peak in many catchments (Duethmann et al., 2015; Gan et al., 2015), and in some cases should remain stable for a few decades (Prasch et al., 2013). In some areas, the glacier runoff peak probably has already passed (Huss and Hock, 2018).

Cryosphere dynamics affect not only the water cycle, but also the sediment cascade and geomorphological evolution of mountain catchments and channels (Lane et al., 2017; Marchese et al., 2017). Unfortunately, the effects of global warming on river sediment fluxes – including both the coarse (moving as bedload) and the fine (transported in suspension) fractions – are much less understood compared to purely hydrological processes (Raymond Pralong et al., 2015; Mao et al., 2019). In the context of current climate change variability, permafrost degradation seems to be responsible for more frequent and larger mass wasting and debris flow events at higher elevations (Gobiet et al., 2014), thus increasing the sediment supply from the hillslopes to the channel network with potentially hazardous consequences on river bed elevations and geometry (i.e. aggradation and widening). Sediment supply to stream channels is also likely augmented by the rapidly developing proglacial areas as well as by more efficient intra- and sub-glacial drainage systems (Swift et al., 2002). Glacier retreat could also increase sediment availability by re-connecting sediment sources at the basin scale (Lane et al., 2017) and by increasing the frequency of glacial lake outburst floods (Iribarren Anacona et al., 2015). Conversely, local morphological conditions may favor – after glacier recession – the formation of proglacial lakes acting as disconnections in sediment transfer, thereby reducing the supply of coarse sediment downstream, potentially triggering bed incision in the channel network (Carrivick and Heckmann, 2017; Lane et al., 2017).

As to the role of glacier dynamics on sediment transport, the effectiveness of subglacial water flow to erode bedrock has already been included in glacier models (e.g. Beaud et al., 2016) and the hydraulics connected with supercooling of subglacial channels has been studied theoretically and numerically (e.g. Creyts and Clarke, 2010), as well as the development and evolution of subglacial drainage networks (Werder et al., 2013). However, field data are still lacking. Remarkably, our understanding of sediment transport dynamics in glacierized river catchments is almost completely limited to the fine fraction in suspension, because few researchers have monitored bedload in such environments (Mao et al., 2019), despite its importance in modifying river morphology.

Recently, the combined use of DoD (DEM of Difference) techniques and sediment flushing data was deployed in a glacierized catchment in Switzerland (Lane et al., 2017), and the integrated use of direct and indirect bedload monitoring was carried out in Norway (Beylich & Laute, 2015), Switzerland (Schneider et al., 2016), Austria (Rickenmann, 2018), Chile (Mao et al., 2016), in addition to Italy (see section 2). However, a quantitative link between bedload rates and related hydrological "drivers" (runoff source) has not been developed yet. Indeed, runoff source (e.g. snowmelt, glacier melt, rainfall) can effectively help identify the main processes by which sediment is transferred from the catchment to the outlet, as well as the main sources of sediments transported within the catchment. As a consequence, it is still not possible to produce reliable, process-based evolutionary scenarios for mountain rivers worldwide, despite the available hydrological predictions (see e.g. Raymond Pralong et al., 2015).

The working hypotheses underlying our research are as follows: i) bedload transport in glacier-fed rivers behaves similarly to suspended sediment in terms of seasonality (imparted by runoff origin) and is thus largely supply-controlled; ii) quantitative relationships between bedload concentration and glacier melt runoff fraction can be established, reflecting the different origin of sediment supply; iii) bedload yield in high-elevation glacierized catchments originates predominantly from glacial areas (sub- and supra-glacial) and is strongly driven by summer air temperature.



## 2 Materials and Methods

### 2.1 Study area

The upper Saldur/Saldura River is a glacierized basin (61.7 $km^2$) located in the Eastern Italian Alps (Fig. 1 and 2). The catchment ranges in elevation between 1632 m a.s.l. at the outlet (village of Matsch/Mazia) and 3725 m a.s.l., and a small glacier (2.2 $km^2$) is present in the upper part of the catchment. The climate is continental and characterized by relatively low annual precipitation (800–1000 mm at 2000 m a.s.l.) usually falling as snow from November to April. This catchment can be considered paradigmatic of many glacierized catchments of the European Alps in terms of geological substrate (dominated by Paleozoic metamorphic basement) and geomorphological setting. The basin was entirely glaciated during the Pleistocene and glacial erosion imparted the typical U-shaped form of the upper basin (Fig. 2). Due to the low amount of liquid precipitation falling during the summer months, the annual runoff is dominated by melt flows from the winter snowpack and the glacier body (Penna et al., 2017). The longitudinal profile of the river is also quite typical, displaying a series of valley steps. Channel pattern ranges from narrow bedrock gorges to wide braided reaches, but it is mostly single-thread featuring a stepped, semi-alluvial morphology (Mao et al., 2014).

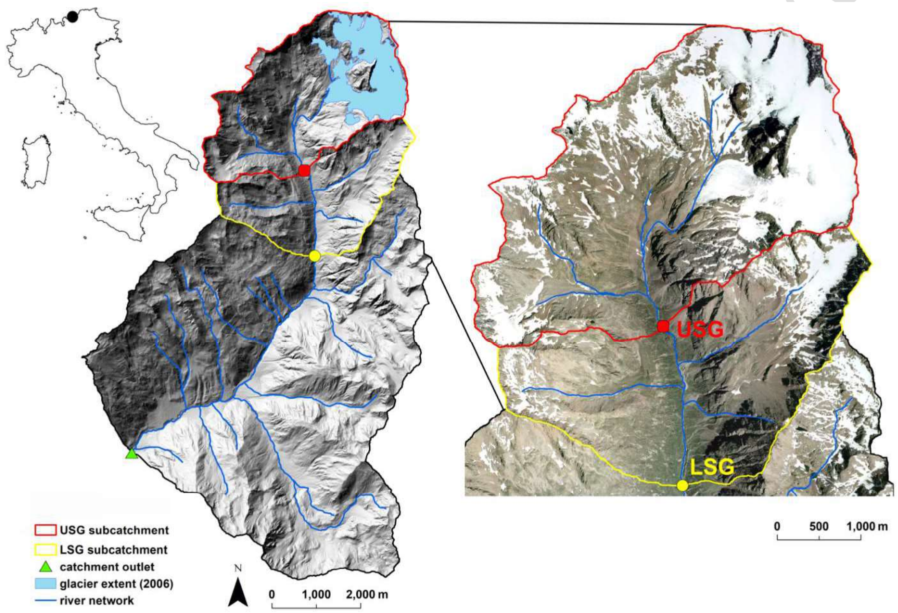


**Figure 1 – Location and map of the Saldur River catchment, showing monitoring sections USG and LSG. Additional images are shown in the supplementary information.**

In the Saldur River, runoff and sediment transport have been monitored since 2011. An array of different methodologies to measure bedload transport have been deployed, encompassing PIT-tagged clast tracking (Mao et al., 2017), acoustic pipe sensor (Dell'Agnese et al., 2014; Mao et al., 2014), and direct sampling ("Bunte" portable traps, Dell'Agnese et al., 2014). In parallel, hydrological tracers (electrical conductivity (EC) and stable isotopes of oxygen and hydrogen) were used to understand timing and relative contribution to runoff of different water sources, in particular snowmelt and glacier melt (Penna et al., 2014; Engel et al., 2016; Penna et al., 2017). Snow cover dynamics were also investigated by means of remote sensing and numerical modelling (Engel et al., 2017).

**Figure 2 –Aerial view of the upper Saldur catchment, with glaciers still mostly covered with snow in July. The location of USG section is marked with a yellow dot. Photo courtesy of the Aut. Province of Bozen-Bolzano.**



## 2.2 Sediment transport monitoring

Bedload samples were collected in the summers of 2011-2014 at section USG (upper stream gauge, drainage area 11 km$^2$, channel slope S=6.8%) and LSG (lower stream gauge, drainage area 19 km$^2$, channel slope S=6%). At both sections, water stage was monitored at a 10-min interval by two pressure transducers, then converted into runoff by using stage-discharge relationships based on salt dilution discharge measurements (see Fig. S1 for the flow rating curve at USG). At LSG, bedload traps (4 mm mesh size, 20x30 cm opening, Bunte et al., 2004) were deployed simultaneously at 2-3 positions across a 5.3 m wide section (Fig. S2), whereas at USG

(4.4 m channel width) traps were installed at 1-2 positions (Fig. S3). The total and unit bedload transport rates for the entire cross-sections ($Q_s$ and $q_s$, respectively) for each sampling period (ranging from 3 to 10 min) were then estimated as width-weighted averages based on the available positions sampled, as presented in Dell'Agnese et al. (2014).

Bedload rates were estimated at LSG (n=105) from 2011 to 2014, and at USG (n=33) from 2012 to 2014. Bedload samples collected at USG were taken at the same exact time of those at LSG (from 10 am to 6 pm, i.e. during the rising limb of melt runoff hydrographs). Bedload samples were subsequently dried, sieved and weighed to obtain the grain size distribution and characteristic diameters. Errors associated with bedload rates for both sections are estimated to be <30%, based on the observed variability in bedload transport during sampling. Values of unit stream power, ω, associated to each bedload sampling at USG and LSG were calculated based on the following equation:

$$\omega = \gamma QS/W \quad (1)$$

where γ is the specific weight of water (assumed constant and equal to 9810 N $m^{-3}$), Q is the water discharge, S is the channel slope, and W is the channel width. Bedload concentrations (in kg $m^{-3}$) were calculated by dividing total bedload rates by the associated water discharges. Suspended sediment transport data were collected from 2012-2014 at LSG through a fixed turbidimeter. Turbidity data were related to suspended sediment concentration (in g $l^{-1}$) by means of direct samples (n=20) which were analysed in the laboratory by filtering, drying and weighing.

### 2.3 Hydrograph separation for runoff origin

At both sections, in 2012 and 2013, stream water sampling was carried out manually (grab samples, n=31 for LSG, n=21 for USG) simultaneous with bedload sampling. For these water samples, EC and stable isotope composition were measured, allowing us to discern the different runoff origins for each bedload sample through hydrograph separation. EC was measured using a portable conductivity meter with instrumental precision of ±0.1 $\mu S\ cm^{-1}$. EC was corrected by a nonlinear temperature compensation at 25 °C. The $\delta^{18}O$ isotopic composition of stream water samples was determined by an isotope ratio mass spectrometer. The isotopic composition of each sample was derived from three repetitions and the standard deviation was computed. The instrumental precision for $\delta^{18}O$ was ±0.2‰. The isotopic composition of snowmelt, glacier melt and groundwater (from selected springs) samples, necessary to perform three-component hydrograph separation, was determined by an off-axis integrated cavity output spectroscope following the procedure reported by Penna et al. (2010, 2012). The instrumental precision for $\delta^{18}O$ was 0.08‰.

Storm events are not considered here as bedload sampling was carried out during dry days, so that the total discharge Q at both USG and LSG can be written as:

$$Q = Q_{gw} + Q_{sm} + Q_{gm} \quad (2)$$

where $Q_{gw}$, $Q_{sm}$ and $Q_{gm}$ represent the groundwater, snowmelt and glacier melt discharge components, respectively, and assuming other possible streamflow components as negligible. As mentioned above, the role of rainfall on the total annual runoff is small in this glacierized catchment, although short-duration, storm-related floods may occur in summer (Engel et al., 2016). For suspended sediment, it was possible to estimate that < 20% of the annual suspended yield is associated with rainfall events in the Saldur catchment (see supplementary material). Therefore, we assume that bedload yields related to storm flows are also a minor component in the long term compared to snowmelt and glacier melt. Furthermore, groundwater flows are not responsible for bedload transport, so the distinction of sediment transport due to snowmelt from glacier melt is the key issue.

The uncertainty related to the three-component hydrograph separation was calculated for glacier melt and groundwater by varying the values of all end-members by ±1 standard deviation, while the uncertainty of high-elevation snowmelt was expressed as the instrumental precision. For glacier melt, uncertainties are <20%. For more details about the hydrograph separation methodology and end-members definition see Engel et al. (2016) and Penna et al. (2017).

### 2.4 DoD analysis and weir flushing data

Based on the availability of two high-resolution, aerial LiDAR-derived terrain models from 2005 and 2013, a DoD analysis was performed on the whole LSG catchment excluding glaciers and ice-cored debris to avoid accounting variations due to ice melting (Fig. S5). For comparability purposes, the 2013 Digital Terrain Model (DTM), originally at 1 m resolution, was resampled by averaging elevation values to obtain the same resolution of the 2005 DTM (2.5 m resolution). In order to reduce the impact of uncorrected alignment between 2005 and 2013 data sets on DoD analysis, both 2.5 m DTMs were converted into two point clouds that were registered using the Iterative Closest Point method of the free software Cloud Compare (http://www.danielgm.net/cc/).

The algorithm was first applied to a stable area to derive a transformation matrix that was then used to align the 2005 data to the more accurate 2013 point cloud. The re-aligned 2005 point cloud was then interpolated to recreate the 2005 DTM to be used in the DoD analysis. In order to account for uncertainty in the analysis, a key issue especially when comparing DTMs of different quality and accuracy (Cavalli et al., 2017), we identified a level of detection (LoD) based on the DoD uncertainty estimated as the standard deviation of errors on selected stable areas (about 60 cm). The threshold error was considered in all DoD cells to derive a map of significant elevation change and calculate volumes of erosion and deposition. In addition, morphological monitoring was carried out by traditional, repeated topographic surveys (12 cross-sections from LSG to the braided proglacial area upstream of USG, see Mao et al., 2014) and by photographic documentation taken from fixed locations to detect changes in the main channel, from 2012 to 2016.

Finally, we investigated temporal changes in sediment transport by taking advantage of flushing operation data from a hydropower weir built in the 1950s on the Saldur River (elevation ~1600 m a.s.l., downstream of the catchment outlet shown in Fig. 1). The data include the number and time of year, beginning in the 1970s, of sediment purges from the settling basin (60 m long, 6 m wide, 5 m deep). Although this information cannot be used to accurately estimate the sediment yield (as in Lane et al., 2017, because trapping efficiency decreases at the higher flow stages due to the weir geometry), the interannual variations in the number of flushing operations provide insight into the long-term changes in sediment transfer along the river.

## 3 Results

### 3.1 Intra-summer variation in sediment transport

Results from the Saldur River indicate that the relationship between sediment transport and water discharge (and thus unit stream power, see Eq. 1) is strongly time-dependent (Fig. 3). Both unit bedload rates ($q_s$) and suspended sediment concentration (SSC) are consistently much higher (up to 5-6 orders of magnitude) during late summer (August and September) than during early summer months (June-July) for identical unit stream power values. It is important to note that all the bedload data refer to days without rainfall, whereby channel runoff is derived from either groundwater, snowmelt and/or glacier melt.

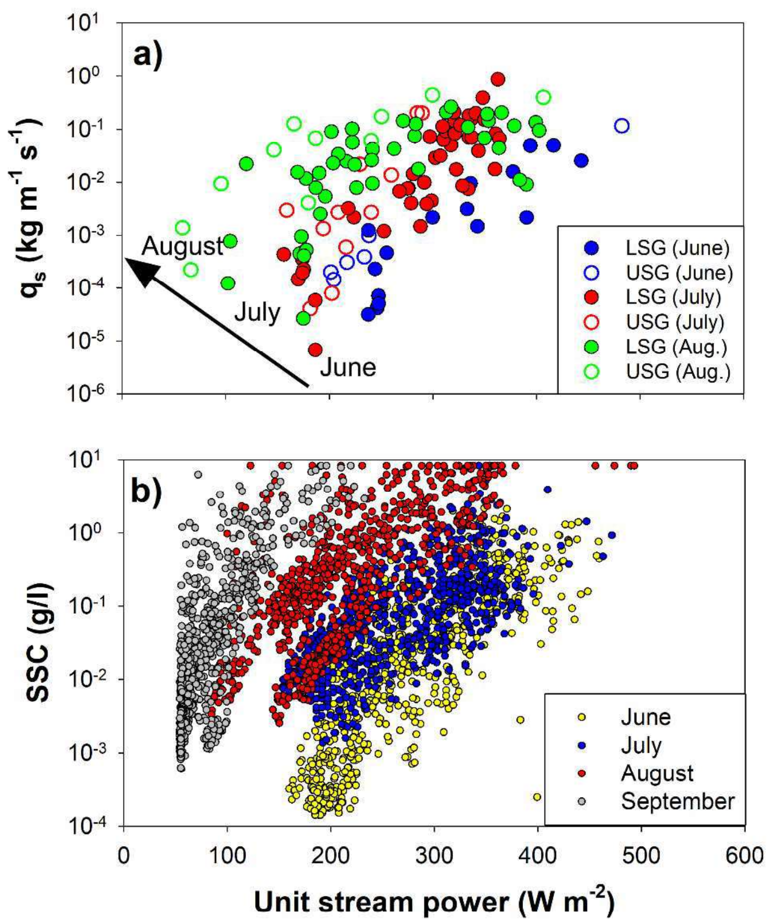


**Figure 3 – Intra-summer variations in (a) bedload rates (per unit of channel width) measured at both LSG and USG in the Saldur River catchment and (b) in suspended sediment concentration (SSC) measured at LSG. The arrow indicates the trend of change during the summer.**

A progressive upward shift in the sediment transport–water flux relationship during the summer is evident (Figures 3a and 3b), whereby high SSC and bedload rates were also measured at the lower water flows in August/September. In contrast, suspended and bedload sediment transport are close to zero for relatively high stream power values in June (Figures 3a and 3b). Such a relationship is not surprising for suspended transport where the supply of sediment is well known to control SSC and thus loads, but it contributes to the increasing evidence of similar controls for bedload as well.

The potential role of grain size on bedload transport rates was then investigated (Fig. 4). We noted that differences in space (USG vs LSG) and time (June to August) in bedload-transported grain size are minor. Overall, the small differences in transported grain size from June to August cannot explain the large increase in bedload rates measured for the same period.

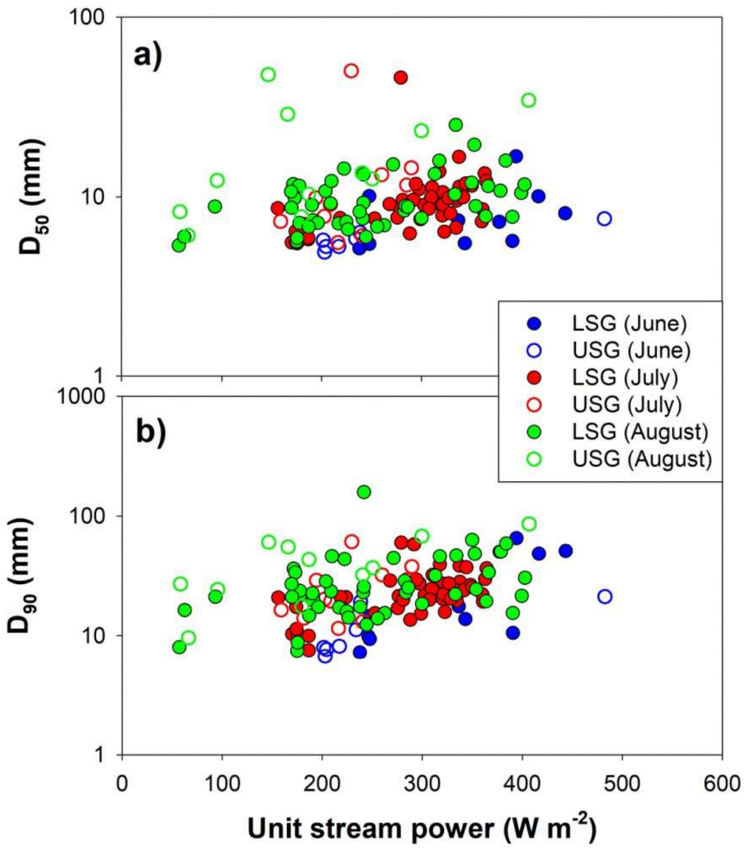


**Figure 4 – Grain size distribution characteristic diameters D50 (a) and D90 (b) of the bedload samples collected in the Saldur River, at sections downstream (LSG) and upstream (USG).**

### 3.2 Runoff origin and bedload transport

The finding that bedload transport rates – for similar water discharge – are much lower in early summer compared to late summer suggests that the runoff origin plays a key role in determining sediment availability. In early summer (typically until mid-late June), the glacier surface is still covered with snow (Engel et al., 2017) and thus the glacier melt fraction is very small to null, and the bulk of river runoff derives from snowmelt (Penna et al., 2017; Zuecco et al., 2019). It is worth highlighting that during this period the glacier outlet is filled with snow, and the outflow from the glacier snout is very small. Indeed, snowmelt runoff from the glacier reaches the downstream channel moving mostly at its surface and by feeding rills spreading on the lateral moraines. As the snowpack on the glacier disappears, the glacier melt contribution rises and surpasses snowmelt in approximately August. As a consequence, the relative proportion of glacier meltwater over the total water discharge ($Q_{gm}/Q$, see Eq. 2) during the bedload sampling times can be used to determine whether the large differences in bedload rates and bedload concentrations (i.e. sediment weight per volume of water) are related to the different runoff sources (i.e. snowmelt vs glacier melt).

The resulting pattern is shown in Figure 5, where bedload concentrations are directly associated with the relative contribution of glacier melt flows in the upper Saldur River. Three important observations can be gathered from this graph: i) bedload concentrations vary by several orders of magnitude for the same river section (USG and LSG) and strongly increase with increasing proportion of glacier melt; ii) the fraction of glacier melt explains a large proportion of the variance in bedload concentration, but iii) annual variations in the relationship and scatter between glacier melt fraction and bedload concentrations are present. Based on a best-fit exponential regression, $R^2$ equals 0.59, 0.97 and 0.60 for 2012, 2013, and 2012-2013 combined, respectively. Accordingly, standard errors of the estimate range from 1 to 7. Power law regression curves were also explored, but they returned slightly lower $R^2$ values. For 2013, the year for which the widest range of glacier melt fraction is available, the best-fit exponential equation combining USG and LSG data ($R^2$= 0.80) is:

$$bc = 0.001\ e^{0.131gm} \quad (3)$$

Where bc is the bedload concentration (in kg $m^{-3}$) and gm is the fraction of glacier melt (in %).



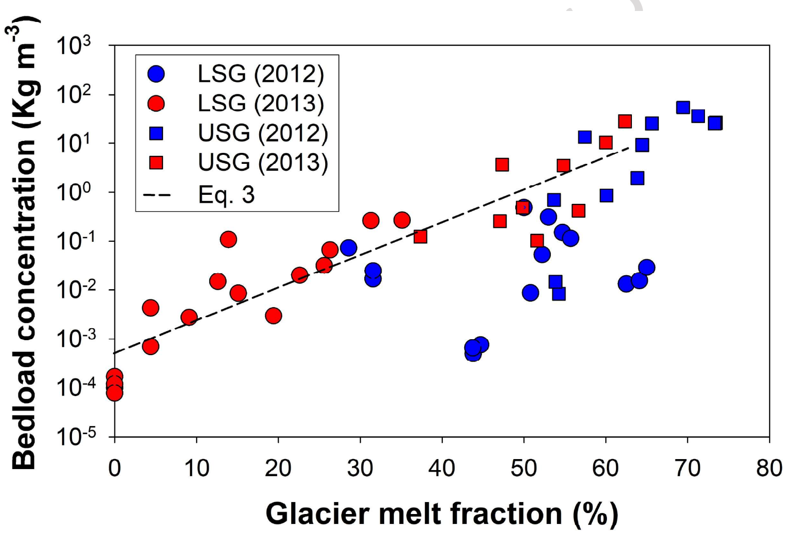


**Figure 5 – Bedload concentration as a function of the glacier melt fraction in the upper Saldur River as estimated through tracers (EC and stable water isotopes) during summer in 2012 and 2013. Uncertainty in**

**the estimated fractions of glacier melt in stream water ranges at USG between 2 and 10%, and at LSG between 1% and 11%. See Figure S4 for a plot of bedload concentration versus the total water discharge.**

### 3.3 Where does bedload come from?

At the short time scale (hourly to daily), the comparison of bedload fluxes measured concurrently at the two cross-sections, USG and LSG, can inform about downstream variations in bedload supply (Fig. 6) and thus on coarse sediment origin. If USG rates are systematically lower than at LSG, then additional sediment sources are expected along the channel from USG to LSG. Conversely, if bedload rates at LGS are consistently lower than at USG, then (at least temporary) deposition along the channel is expected between the two sections. After having estimated bedload rates for the two cross-sections, the plot shown in Figure 6 is obtained.

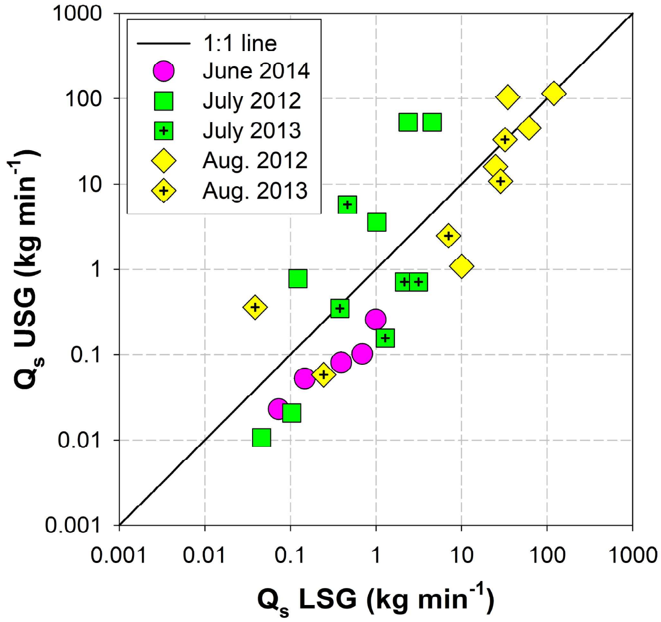


**Figure 6 – Comparison of concurrent bedload fluxes at USG and LSG sections. Only a subset of the entire bedload dataset is shown, when concurrent measurements of bedload rates were taken at both USG and LSG (in 2012, 2013 and 2014).**

Data points lie both below (bedload at LSG larger than at USG) and above (bedload at USG larger than at LSG) the perfect agreement line. Interestingly, August data (glacier melt flows) are those mostly falling closer to the 1:1 line, whereas June data (snowmelt-driven flows) indicate that bedload rates were greater at LSG than at USG. July data (during periods of mixed snowmelt and glacier melt inputs to the river) feature the largest scatter, falling both below and above the 1:1 line. A closer inspection of these data reveals that July 2012 points tend to fall above the line and those from July 2013 below. The changes in sediment supply conditions from

June to August and from year to year – depicted in Figures 3 and 5 – seem to be confirmed also by such variations in the longitudinal sediment transfer balance. During the highest bedload rates typical of August glacier melt period, a substantial longitudinal equilibrium in bedload transport – coarse sediment passing through USG is entirely transferred down to LSG – is apparent, indicating that bedload material at the outlet originates from upstream of USG at the glacier. Indeed, no other sediment sources were observed to be active in this period. Substantial variations in either bed morphology or channel banks were not observed, and the few tributaries do not contribute coarse bedload (>4 mm) transport during the sampling periods. Indeed, these tributaries mostly transport large quantities of sand, likely as as consequence of the presence of longitudinal disconnections (i.e. terminal moraines creating proglacial lakes and plains).

However, to address the issue of sediment sources at longer (multiannual) time scales and at wider spatial scales (across the whole basin area), the morphological changes over the entire basin become important. The frequency distribution of geomorphic changes derived from the 2005-2013 DoD analysis is shown in Figure 7, and the spatial pattern in Figure 8.



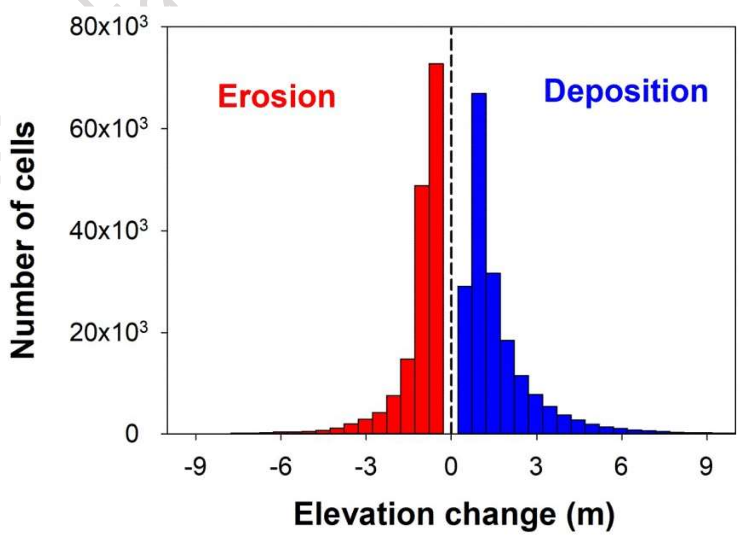


**Figure 7 – Frequency distributions of geomorphic changes in the Saldur basin, obtained by the DoD analysis.**

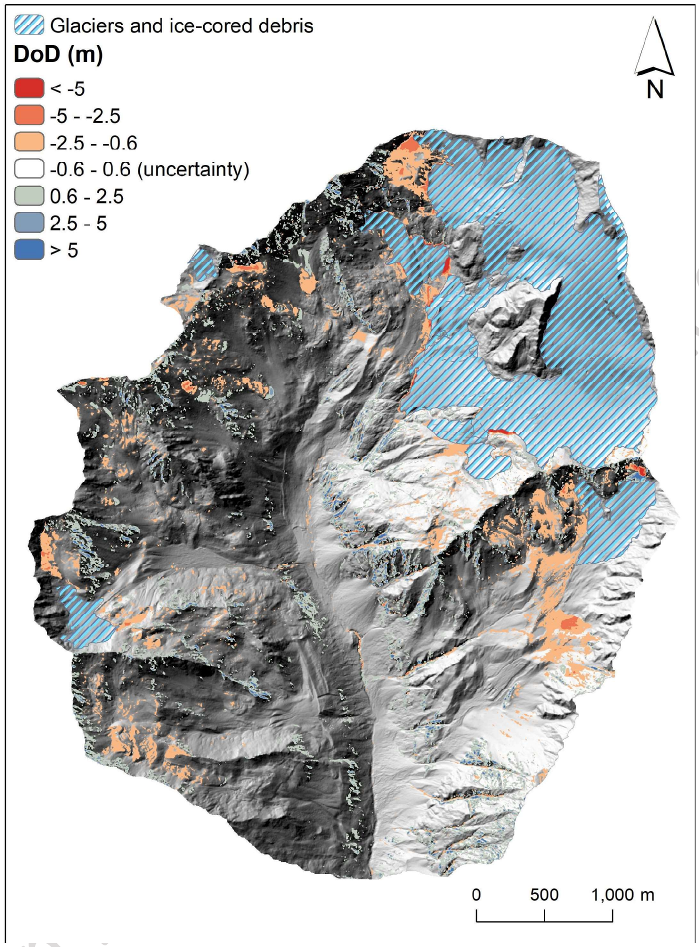


**Figure 8 – DoD map of geomorphic changes that occurred in the upper Saldur catchment between 2005-2013. Glaciers and ice-cored debris were areas excluded from the analysis. See Figure S5 for a close up of the lower part of the catchment.**



The area of detectable changes (i.e. above threshold) is 16% of the investigated area, which in terms of absolute area, is 2,136,360 $m^2$, i.e. about 2 $km^2$. The total erosion volume is 1,146,220 $m^3$ (±590,190 $m^3$), whereas deposition is 1,923,340 $m^3$ (±691,620 $m^3$). The net volume difference indicates a net deposition in the catchment of about 777,000 $m^3$ but with a similar error (about ± 900,000 $m^3$) indicating that averaged vertical changes are actually small (0.06 m, with an error of ± 0.07 m). Restricting the vertical variations to the areas in which elevation changes actually occurred, the net average deposition is about 0.36 m (with ± 0.43 m error). Based on the thresholded DoD analysis, the imbalance (departure from equilibrium) indicates deposition (13%) but with a large degree of uncertainty, whereas a raw, unthresholded analysis returns a -1% imbalance. Overall, and considering the magnitude of the DoD uncertainty, the sediment cascade processes in the Saldur catchment outside of the glacial domain appear to be generally balanced between erosion and deposition. Given the adopted threshold (±60 cm) and the negative (i.e. erosion) net volume difference of the unthresholded analysis, we argue that most of the distributed erosion in the catchment was characterized by values lower than the error threshold and hence excluded from the final budget. Only the more concentrated erosion patterns were captured by the analysis. Also, depositional patterns in the catchment appear to be quite spatially distributed, and small in area. Deposits are instead mainly localized in the lower parts of the hillslopes and mostly quite far from the main channel network, which thus appears to be substantially disconnected from mass wasting processes (Fig. 8).

Indeed. such an approximate balance between erosion and deposition is also true for the main river channel, where – beside the DoD analysis – the annual comparison of 12 cross-sections and repeated photographs indicate overall river bed stability, both vertically and laterally, with changes in the order of few centimeters (i.e. about the $D_{50}$ of the channel bed). Bank erosion was very limited, and the channel was stable both in planform and in elevation. The only exception (see Fig. S5) is a narrow, bedrock-confined reach showing incision (where accessibility for cross-section surveys was absent), and about 100 m at the confluence with the most active fan of the catchment, where localized deposition did occur. Therefore, the main channel is presently in equilibrium despite the relevant annual sediment load (~$10^3$ $m^3$ of bedload and ~$10^4$ $m^3$ of suspended load, estimated from season-based rating curves). As a consequence, the net sediment load estimated at LSG must have originated from the glaciarized portion of the basin, i.e. the area subtracted from the DoD analysis which included the actual glaciers and the evident ice-cored debris at their margins. The proglacial reaches already exposed in 2005 did not undergo significant changes. It is therefore quite remarkable how sediment volumes eroded and deposited within the catchment – assessed by the DoD analysis – outweighs by one order of magnitude the estimated sediment yield of the catchment, once more highlighting the role of (dis)connectivity in mediating the transfer of hillslope processes to the outlet.



**3.4 Sediment export and climate**

The analysis of flushing frequencies in the settling basin relative to the hydropower weir located on the Saldur River a few kilometers downstream of LSG allows insights into the decadal variations in sediment transport, and the likely connections with climatic conditions. Figure 9a displays a clear trend in the temperatures relative to potential sediment transport periods (June to October), but with large inter-annual variations. The number of flushing operations per year peaked in the late 1990s-early 2000s, suggesting a direct link with temperatures and no relation with precipitation during those months. Indeed, Figure 9b illustrates the positive but scattered relation (Spearman correlation $R=0.43$, $p<0.01$) between flushing number and temperature. However, when single decades are investigated, more definite trends emerge (e.g. 1990s, 2000s). Conversely, the analysis of flushing operations versus precipitation does not show any statistically significant correlation, also considering different periods of the year. About 60% of all the flushing operations from 1977 to 2015 occurred between July and September, with only about 25-30% taking place in June (Fig. 10), although this month is characterized by the highest runoff associated with snowmelt (Penna et al., 2017). These results again point to the dominant role of glacier melt flows in determining the sediment yield of the Saldur River.

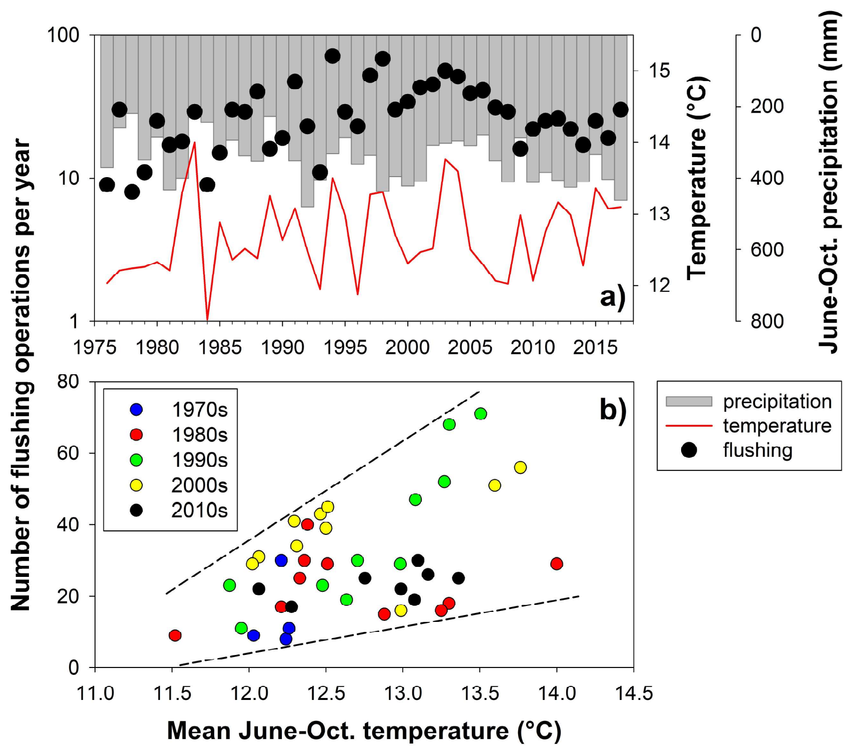


**Figure 9 – Temporal trend (a) of the number of flushing operations per year at the hydropower weir and mean air temperatures (June to October) measured at the outlet, and (b) their relationship binned into the fferent decades. Upper and lower envelope curves (fitted by eye) are shown to highlight the different influences of temperature on minimum and maximum flushing frequencies.**

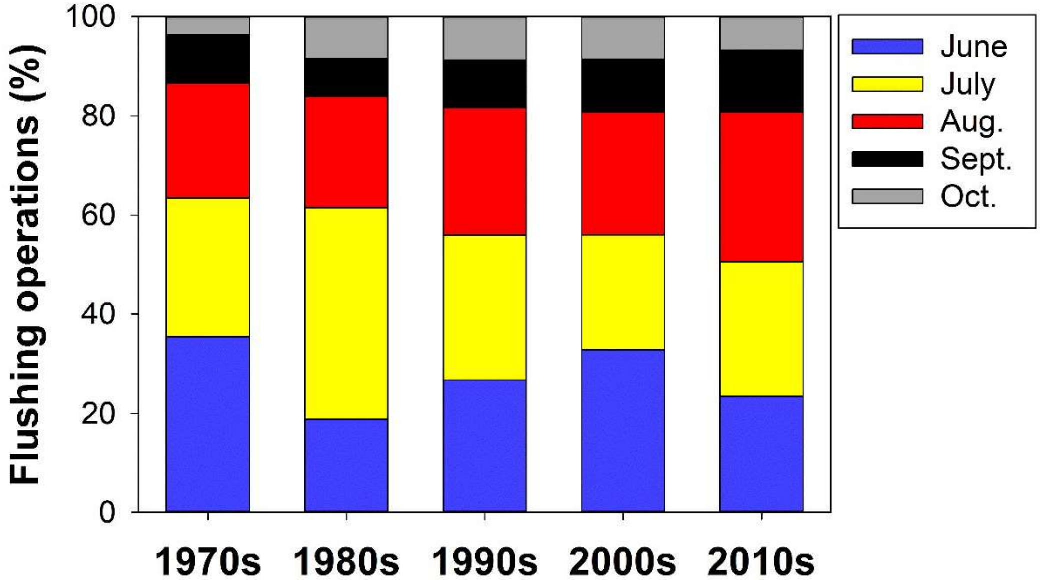


**Figure 10 – Relative monthly distribution of flushing operations in the Saldur River from 1970s to 2010s. Flushing from July to August (when runoff includes a large share of glacier melt) prevail the annual distribution, although June (snowmelt runoff, very little glacier melting) typically features the highest runoff volume of the year (Penna et al., 2017).**

## 4 Discussion

To the best of our knowledge, this is the first study that combined runoff origin analysis with bedload estimation in mountain catchments. Our application establishes an explicit link between bedload sediment dynamics and water runoff origin in the Saldur River basin, which is paradigmatic of many glacierized catchments in the Alps as well as of other mountain ranges where water runoff is dominated by cryosphere-related processes due to relatively low summer precipitation. The results of our investigations confirm our three working hypothesis, as summarized below.

*Bedload transport is strongly supply-controlled and is season-dependent.* The compelling evidence emerging from our large bedload dataset that bedload transport is supply limited is not novel itself, given that steep (>3-5%) mountain channels are long known to be so (Comiti &

Mao, 2012). Nonetheless, most numerical modelling studies still apply bedload transport capacity equations that assume full sediment availability and do not account for supply limited conditions (e.g. Raymond Pralong et al., 2015). In the Saldur River, widely used equations for quantifying bedload rates in mountain rivers overestimate from 1 to 4 orders of magnitude for near bankfull stages in August to lower stages in June, respectively, even with form drag corrections applied (Rickenmann, 2012). We documented over 5 orders of magnitude variations in bedload rates occurring from June to August, for similar water discharges in the absence of relevant changes in transport sediment size. In other words, bedload concentrations increase from snowmelt to glacier melt periods very much in the same way as suspended transport does, indicating that sediment supply increases over summer both in terms of fine and coarse (>4 mm) particles. Large variability in bedload transport rates for unit stream powers of around 100 - 200 $W/m^2$ were previously documented in other comparable streams (Bunte et al., 2008; Church, 2010). More recently, the use of surrogate methods (geophone and impact plates) for bedload monitoring (Hilldale, 2015; Rickenmann, 2016; Downs et al., 2016; Aigner et al., 2017), also including glacier-fed streams (Rickenmann, 2018), expands the range of variability in bedload transport rates up to unit stream powers of 500 $W/m^2$ . However, this is the first time that large seasonal changes in bedload rates are precisely related to runoff origin.

*Bedload concentration is related to glacier melt runoff fraction.* The higher bedload concentrations measured in August are strongly related to glacier melting at the time of sampling (Fig. 5), which also reflects the effect of the subglacial network development and thus the higher supply of coarse sediments from the base of the glaciers, which is not accessible to the snowmelt runoff. However, our results show that there is a more complex relationship between the two variables, as bedload varied substantially from 2012 to 2013 for intermediate glacier melt fractions. Although one of our goals was to develop general quantitative relationships (at least for the Saldur River), the fact that each year features different responses between glacier melt and bedload transport is reasonable. In fact, the expected sediment sources as well as sediment connectivity to the channel evolve through time (Carrivick & Heckmann, 2017). Thus, for the same proportion of glacier melt in the river, very different bedload supply rates and thus concentrations develop. Additionally, it is important to highlight that the observed strong link between glacier melt and bedload transport does not imply that the sediment clasts sampled at USG and LSG were actually sourced directly from the glacier, without any intervening storage. Virtual particle velocities assessed in the Saldur River (Mao et al., 2017) indicate that bedload transit times in the study reaches are much longer than for water runoff, and thus the relationship between glacier melt and bedload concentration is likely due to an increased bed mobility associated with an augmented bedload supply (as found by Venditti et al., 2010; Ancey et al., 2015; Kammerlander et al., 2017).

*Bedload in glacierized catchments originates mostly from glacial areas.* The DoD results combined with the observed channel bed equilibrium indicate that the most important sediment sources for bedload transport at the annual to multi-annual scale lie within the glacierized and dead ice-cored portion of the basin, notwithstanding the large sediment volumes eroded from the hillslopes that are transferred downslope only locally without reaching the channel network. This finding matches our hydrological analysis and suggests that the role of liquid precipitation in sediment transfer in similar “dry” inner mountain basins is minor. As in other glacierized environments, high sediment supply can indeed be provided by highly dynamic subglacial channels (Swift et al., 2002; Kulessa et al., 2008). Nonetheless, intense coarse sediment transport was observed in supraglacial channels on the main Saldur glacier in late summer (see video in the supplemental information). Basically, the Saldur River in the present times of assumed nearly-maximum runoff appear to work mainly as a “conveyor belt” (although there is a continuous sediment exchange at the particle scale) for all the sediment eroded from the upper part of the catchment by glacial processes, as runoff bedload capacity largely exceeds the sediment volumes supplied annually by the catchment. Finally, the sediment export at multi-decadal scale – based on weir flushing frequency – is linked to summer air temperature and not to precipitation trends, with most of flushing operations occurring in July-August, again confirming the dominant role of glacier melt on the long-term sediment dynamics. However, the fact that sediment flushing frequency has been decreasing since the late 1990s despite very warm summers in the following decades – including exceptional heat waves as in 2003 and 2017 – highlights the unsteady nature of sediment supply from the glaciers as they recede, and underscores the complexity of these fast-evolving systems.

## 5 Conclusions

Higher temperatures in mountainous regions worldwide are determining changes in the hydrologic regime of glacierized catchments, but little is known about how sediment transport in such catchments is responding. Understanding where the sediment comes from and its timing has important implications for predicting future morphological and ecological variations. Our results obtained from a glacierized basin in the Alps indicate that water runoff origin plays a key role in sediment transport dynamics, with both fine and coarse fractions of sediment moving predominantly during glacier melt. Moreover, sediments are largely sourced from within the glacier-covered portion of the basin.

Modelling studies foresee a reduction in annual water runoff for Alpine glacierized catchments similar to the Saldur starting from the 2020s, and possible disappearance of glaciers by the end of the century (Gobiet et al., 2014). The decreased bedload-transporting runoff will be mostly determined by reduced glacier melt flows associated with shrinking ice masses (Raymond Pralong et al., 2015). As a consequence, bedload supply from the glacier will also likely diminish; large areas of the upper catchment – presently glaciarized – will become covered by unconsolidated sediment while others will be exposed bedrock. In the next decades, trends in sediment transport will strongly depend on changes in surface sediment connectivity due to glacier retreat (Cavalli et al., 2019) as well as on subglacial terrain morphology and the actual availability of sediment at the base and on the surface of the receding glacier. In parallel, degrading permafrost will probably lead to higher mass wasting processes, potentially increasing the availability of unconsolidated sediment in the upper catchment. We thus envisage for the second half of the century, in catchments almost completely deglaciated, a shift from current glacier-driven, supply-limited conditions to transport-limited dynamics where episodic, storm-related floods will dominate bedload transfer by eroding the newly available sediments. Nonetheless, actual sediment supply to the channel network may be locally quite variable, depending on the connectivity of the freshly exposed sediment sources with the channel network.



**Acknowledgments**

This work has been possible thanks to different research projects focusing on the Saldur basin (which corresponds to the LTSER macrosite “Mazia/Matsch”, coordinated by EURAC

Research): “EMERGE” granted by the Dr. Erich-Ritter-Stiftung and the Dr. Herzog-Sellenberg-Stiftung (Germany); “Effects of climate change on high-altitude ecosystems: monitoring the Upper Matsch Valley”, granted by the Free University of Bozen-Bolzano, and “GLORI” granted by the Aut. Province of Bozen-Bolzano. Support for S. Rathburn was provided by National Science Foundation award IIA-1361496. Bedload dataset is available as SI. Johannes Holzner is acknowledged for the analysis of weir flushing data, which have been kindly provided by the company “Alperia S.p.A.”. Precipitation data have been provided by EURAC Research – Institute of Alpine Environment (courtesy of Georg Niedrist and Giacomo Bertoldi). We thank Dieter Rickenmann and an anonymous reviewer for their valuable comments and suggestions that greatly improved the manuscript.



**References**

Aigner, J., Kreisler, A., Rindler, R., Hauer, C., & Habersack, H. (2017). Bedload pulses in a hydropower affected alpine gravel bed river. Geomorphology, 291, 116-127. https://doi.org/10.1016/j.geomorph.2016.05.015

Ancey, C., Bohorquez, P., & Heyman, J. (2015) Stochastic interpretation of the advection diffusion equation and its relevance to bed load transport. *J. Geophys. Res. – Earth Surface,* 120, 2529–2551.

Beaud, F., Flowers, G.E. and Venditti, J.G. (2016), Efficacy of bedrock erosion by subglacial water flow, Earth Surface Dynamics 4, 125-145.

Beniston, M., Farinotti, D., Stoffel, M., Andreassen, L.M., Coppola, E., Eckert, N., et al. (2017) The European mountain cryosphere: A review of past, current and future issues. *The Cryosphere Disc*., https://doi.org/10.5194/tc-2016-290 (2017).

Beylich, A.A., & Laute, K. (2015) Sediment sources, spatiotemporal variability and rates of fluvial bedload transport in glacier-connected steep mountain valleys in western Norway (Erdalen and Bødalen drainage basins). *Geomorphology*, 228, 552-567.

Bunte, K., Abt, S.R., Potyondy, J.P. & Ryan, S.E. (2004) Measurement of coarse gravel and cobble transport using portable bedload traps. *J. Hydraulic Engineering*, 130(9), 879-893.

Bunte, K., Abt, S. R., Potyondy, J. P., & Swingle, K. W. (2008). A comparison of coarse bedload transport measured with bedload traps and Helley-Smith samplers. Geodinamica Acta, 21(1/2), 53-66.

Carrivick, J.L., & Heckmann, T. (2017) Short-term geomorphological evolution of proglacial systems. *Geomorphology*, 287, 3-28.

Cavalli, M., Goldin, B., Comiti, F., Brardinoni, F., & Marchi, L. (2017) Assessment of erosion and deposition in steep mountain basins by differencing sequential digital terrain models. *Geomorphology*, 291, 4-16.

Cavalli, M., Heckmann, T., & Marchi L. (2019) Sediment connectivity in proglacial areas. *Geomorphology of Proglacial Systems. Landform and Sediment Dynamics in Recently Deglaciated Alpine Landscapes*, eds Heckmann T, Morche D, Springer International Publishing, Cham, 271–287.

Comiti, F. & Mao, L. (2012) Recent Advances in the Dynamics of Steep Channels. Gravel-Bed Rivers: Processes, Tools, Environments, eds Church M, Biron PM, Roy AG (Wiley), pp 351-377, DOI: 10.1002/9781119952497.

Church, M. (2010). Chapter 2: Mountains and montane channels. In T. Burt & R. Allison (Eds.), Sediment cascades (pp. 17-53). Oxford, UK: John Wiley-Blackwell.

Creyts, T. T., and G. K. C. Clarke (2010) Hydraulics of subglacial supercooling: Theory and simulations for clear water flows, J. Geophys. Res., 115, F03021, doi:10.1029/2009JF001417.

Dell'Agnese, A., Mao, L. & Comiti, F. (2014) Calibration of an acoustic pipe sensor through bedload traps in a glacierized basin. *Catena*, 121, 222-231.

Downs, P. W., Soar, P. J., & Taylor, A. (2016). The anatomy of effective discharge: The dynamics of coarse sediment transport revealed using continuous bedload monitoring in a gravel-bed river during a very wet year. Earth Surface Proc. Landforms, 41, 147-161.

Duethmann, D. et al. (2015) Attribution of streamflow trends in snow and glacier melt-dominated catchments of the Tarim River, Central Asia. *Water Resour. Res.,* 51, 4727-4750.

Engel, M., Penna, D., Bertoldi, G., Dell'Agnese, A., Soulsby, C., & Comiti, F. (2016) Identifying run-off contributions during melt-induced run-off events in a glacierized alpine catchment. *Hydrological Processes*, 30 (3), 343-364.

Engel, M., Notarnicola, C., Endrizzi, S., & Bertoldi, G. (2017) Snow model sensitivity analysis to understand spatial and temporal snow dynamics in a high-elevation catchment. *Hydrol. Process.*, 31(23), 4151-4168.

Gan, R., Luo, Y., Zuo, Q., & Sun, L. (2015) Effects of projected climate change on the glacier and runoff generation in the Naryn River Basin, Central Asia. *J. Hydrol.*, 523, 240-251.

Gobiet, A. et al. (2014) 21$^{st}$ century climate change in the European Alps-A review. *Sci. Total Environ.*, 493, 1138-1151.

Grosse, G., Goetz, S., McGuire, A.D., Romanovsky, V.E., & Schuur, E.A.G. (2016) Changing permafrost in a warming world and feedbacks to the Earth system. *Environ. Res. Lett*., 11(4), 040201.

Hilldale, R. C. (2015). Continuous bed load measurement with impact plates on the Elwha River, WA. Paper presented at Proceedings of the 3rd Joint Federal Interagency Conference on Sedimentation and Hydrologic Modeling (pp. 418-431). Reno, NV, April 19-23, 2015.

Huss, M., and R. Hock (2018) Global-scale hydrological response to future glacier mass loss. *Nat. Clim. Change*. 8(2), 135-140

Iribarren Anacona, P., Mackintosh, A., & Norton, K. (2015) Reconstruction of a glacial lake outburst flood (GLOF) in the Engaño Valley, Chilean Patagonia: Lessons for GLOF risk management. *Sci. Total Environ*, 527–528, 1-11

Kammerlander, J., Gems, B., Kößler, D., & Aufleger, M. (2017) Effect of bed load supply on sediment transport in mountain streams. *Int. J. Sediment Res*., 32(2), 240-252.Kobierska, F,, Jonas, T., Zappa, M., Bavay, M., Magnusson, J., & Bernasconi, S.M. (2013) Future runoff from a partly glacierized watershed in Central Switzerland: A two-model approach. *Adv. in Water Resour*., 55, 204-214.

Kulessa, B., Booth, A.D., Hobbs, A., & Hubbard, A.L. (2008) Automated monitoring of subglacial hydrological processes with ground penetrating radar (GPR) at high temporal resolution: scope and potential pitfalls. *Geophys. Res. Lett*., 35(24), L24502.

Lane, S.N., Bakker, M., Gabbud, C., Micheletti, N., & Saugy, J.N. (2017) Sediment export, transient landscape response and catchment-scale connectivity following rapid climate warming and Alpine glacier recession. *Geomorphology*, 277, 210-227.

Mao, L., Dell'Agnese, A., Huincache, C., Penna, D., Engel, M., Niedrist, G., & Comiti F. (2014) Bedload hysteresis in a glacier-fed mountain river. *Earth Surf. Process. Landforms*, 39(7), 964-976.

Mao, L., Carrillo, R., Escauriaza, C. & Iroume, A. (2016) Flume and field-based calibration of surrogate sensors for monitoring bedload transport. *Geomorphology*, 253, 10-21.

Mao, L., Dell'Agnese, A. & Comiti, F. (2017) Sediment motion and velocity in a glacier-fed stream. *Geomorphology*, 291, 69-79 (2017).

Mao, L., Comiti, F., Carrillo, R. & Penna, D. (2019) Sediment transport in proglacial rivers. *Geomorphology of Proglacial Systems. Landform and Sediment Dynamics in Recently Deglaciated Alpine Landscapes*, eds Heckmann T, Morche D Springer International Publishing, Cham, 199-217.

Marchese, E., Scorpio, V., Fuller, I., McColl, S. & Comiti, F. (2017) Morphological changes in Alpine rivers following the end of the Little Ice Age. *Geomorphology*, 295, 811-826.

Milner, A.M., Khamis, K., Battin, T.J., Brittain, J.E., Barrand, N.E., Füreder, L., et al. (2017) Glacier shrinkage driving global changes in downstream systems. *PNAS*, 114(37), 9770-9778.

Penna, D., Engel, M., Mao, L., Dell'Agnese, A., Bertoldi, G., & Comiti, F. (2014) Tracer-based analysis of spatial and temporal variations of water sources in a glacierized catchment. *Hydrol. Earth Syst. Sci*., 18(12), 5271-5288.

Penna, D., Engel, M., Bertoldi, G. & Comiti (2017), F. Towards a tracer-based conceptualization of meltwater dynamics and streamflow response in a glacierized catchment. *Hydrol. Earth Syst. Sci.*, 21(1), 23-41.

Penna, D., Stenni, B., Šanda, M., Wrede, S., Bogaard, T.A., Gobbi, A., Borga, M., Fischer, B.M.C., Bonazza, M., Chárová, Z., (2010). On the reproducibility and repeatability of laser absorption spectroscopy measurements for $\delta^2$H and $\delta^{18}$O isotopic analysis. Hydrology and Earth System Sciences 14, 1551–1566. https://doi.org/10.5194/hess-14-1551-2010

Penna, D., Stenni, B., Šanda, M., Wrede, S., Bogaard, T.A., Michelini, M., Fischer, B.M.C., Gobbi, A., Mantese, N., Zuecco, G., Borga, M., Bonazza, M., Sobotková, M., Čejková, B., Wassenaar, L.I., 2012. Technical Note: Evaluation of between-sample memory effects in the analysis of $\delta^2$H and $\delta^{18}$O of water samples measured by laser spectroscopes. Hydrology and Earth System Sciences 16, 3925–3933. https://doi.org/10.5194/hess-16-3925-2012

Prasch, M., Mauser, W. & Weber, M. (2013) Quantifying present and future glacier melt-water contribution to runoff in a central Himalayan river basin. *Cryosphere*, 7(3), 889-904.

Raymond Pralong, M., Turowski, J.M., Rickenmann, D. & Zappa, M. (2015) Climate change impacts on bedload transport in alpine drainage basins with hydropower exploitation. *Earth Surf. Process. Landforms*, 40 1587-1599 (2015).

Rickenmann, D. (2012) Alluvial Steep Channels: Flow Resistance, Bedload Transport Prediction, and Transition to Debris Flows. *Gravel-Bed Rivers: Processes, Tools, Environments*, eds Church M, Biron PM, Roy AG (Wiley), DOI: 10.1002/9781119952497.ch28.

Rickenmann, D. (2016) Methods for the quantitative assessment of channel processes in torrents (steep streams). London, UK: Taylor & Francis. https://doi.org/10.1201/b21306

Rickenmann, D. (2018) Variability of bed load transport during six summers of continuous measurements in two Austrian mountain streams (Fischbach and Ruetz). Water Resources Research, 54, 107-131. https://doi.org/10.1002/2017WR021376.

Schneider, J.M., Rickenmann, D., Turowski, J.M., Schmid, B. & Kirchner, J.W. (2016) Bed load transport in a very steep mountain stream (Riedbach, Switzerland): Measurement and prediction. *Water Resour. Res*., 52(12), 9522-9541..

Swift, D.A., Nienow, P.W., Spedding, N. & Hoey, T.B. (2002) Geomorphic implications of subglacial drainage configuration: rates of basal sediment evacuation controlled by seasonal drainage system evolution. *Sediment. Geol*., 149(1–3), 5-19.

Venditti, J.G., Dietrich, W.E., Nelson, P.A., Wydaga, M.A., Fadde, J., & Sklar, L. (2010) Mobilization of coarse surface layers in gravel-bedded rivers by finer gravel bed load. *Water Resour. Res*., 46, DOI:10.1029/2009WR008329.W07506.

Weber, M. & Prasch, M. (2016) Influence of the glaciers on runoff regime and its change. *Regional Assessment of Global Change Impacts: The Project GLOWA*-Danube, eds Mauser W, Prasch M (Springer), 493-509.

Werder, M. A., Hewitt I. J., Schoof C. G., and Flowers G. E. (2013) Modeling channelized and distributed subglacial drainage in two dimensions. J. Geophys. Res. Earth Surf., 118, 2140-2158. doi:10.1002/jgrf.20146.

Zuecco, G., Carturan, L., De Blasi, F., Seppi, R., Zanoner, T., Penna, D., Borga, M., Carton, A., Dalla Fontana, G., 2019. Understanding hydrological processes in glacierized catchments: evidence and implications of highly-variable isotopic and electrical conductivity data. Hydrological Processes 33:816–832. https://doi.org/10.1002/hyp.13366